



## Synthesis Methods of Two-Dimensional MoS<sub>2</sub>: A Brief Review

Downloaded from: <https://research.chalmers.se>, 2025-07-02 13:58 UTC

Citation for the original published paper (version of record):

Sun, J., Li, X., Guo, W. et al (2017). Synthesis Methods of Two-Dimensional MoS<sub>2</sub>: A Brief Review. Crystals, 7(7): Article no 198 -. <http://dx.doi.org/10.3390/cryst7070198>

N.B. When citing this work, cite the original published paper.

Review

# Synthesis Methods of Two-Dimensional MoS<sub>2</sub>: A Brief Review

Jie Sun <sup>1,2,\*</sup>, Xuejian Li <sup>1</sup>, Weiling Guo <sup>1</sup>, Miao Zhao <sup>3</sup>, Xing Fan <sup>1</sup>, Yibo Dong <sup>1</sup>, Chen Xu <sup>1</sup>, Jun Deng <sup>1</sup> and Yifeng Fu <sup>4,\*</sup>

<sup>1</sup> Key Laboratory of Optoelectronics Technology, College of Microelectronics, Beijing University of Technology, Beijing 100124, China; xuejianli@emails.bjut.edu.cn (X.L.); guoweiling@bjut.edu.cn (W.G.); fanxing111@emails.bjut.edu.cn (X.F.); donyibo@emails.bjut.edu.cn (Y.D.); xuchen58@bjut.edu.cn (C.X.); dengsu@bjut.edu.cn (J.D.)

<sup>2</sup> Quantum Device Physics Laboratory, Department of Microtechnology and Nanoscience, Chalmers University of Technology, Göteborg 41296, Sweden

<sup>3</sup> High-Frequency High-Voltage Device and Integrated Circuits Center, Institute of Microelectronics, Chinese Academy of Sciences, Beijing 10029, China; zhaomiao@ime.ac.cn

<sup>4</sup> Electronics Material and Systems Laboratory, Department of Microtechnology and Nanoscience, Chalmers University of Technology, Göteborg 41296, Sweden

\* Correspondence: jie.sun@bjut.edu.cn (J.S.); yifeng.fu@chalmers.se (Y.F.)

Academic Editor: Filippo Giannazzo

Received: 19 May 2017; Accepted: 28 June 2017; Published: 1 July 2017

**Abstract:** Molybdenum disulfide (MoS<sub>2</sub>) is one of the most important two-dimensional materials after graphene. Monolayer MoS<sub>2</sub> has a direct bandgap (1.9 eV) and is potentially suitable for post-silicon electronics. Among all atomically thin semiconductors, MoS<sub>2</sub>'s synthesis techniques are more developed. Here, we review the recent developments in the synthesis of hexagonal MoS<sub>2</sub>, where they are categorized into top-down and bottom-up approaches. Micromechanical exfoliation is convenient for beginners and basic research. Liquid phase exfoliation and solutions for chemical processes are cheap and suitable for large-scale production; yielding materials mostly in powders with different shapes, sizes and layer numbers. MoS<sub>2</sub> films on a substrate targeting high-end nanoelectronic applications can be produced by chemical vapor deposition, compatible with the semiconductor industry. Usually, metal catalysts are unnecessary. Unlike graphene, the transfer of atomic layers is omitted. We especially emphasize the recent advances in metalorganic chemical vapor deposition and atomic layer deposition, where gaseous precursors are used. These processes grow MoS<sub>2</sub> with the smallest building-blocks, naturally promising higher quality and controllability. Most likely, this will be an important direction in the field. Nevertheless, today none of those methods reproducibly produces MoS<sub>2</sub> with competitive quality. There is a long way to go for MoS<sub>2</sub> in real-life electronic device applications.

**Keywords:** Molybdenum disulfide; transition metal dichalcogenide; two-dimensional materials; micromechanical exfoliation; chemical vapor deposition.

## 1. Introduction

Recently, graphene has received considerable attention in scientific communities. It is recognized as a new wonder material (e.g., record carrier mobility, thermal conductivity, mechanical strength and flexibility), and applications in nanocomposites, paints, transparent electrodes, heat spreaders, etc. are being explored [1]. However, one should not forget that the original motivation for studying graphene was in its field effect [2], with a hope that it might play a key role in nanoelectronics, rather than serving as a passive element such as electrodes [3]. Nevertheless, at this stage, due to the difficulties in

opening an energy bandgap in graphene, it is not clear whether graphene will become a key material in electronics at all. Therefore, the search for other two-dimensional (2D) materials (materials with one or few atomic layers) with an inherent energy bandgap that is suitable to make transistors is essential. Black phosphorus [4], transition metal dichalcogenide (TMD) [5], gallium nitride [6], etc. are extensively explored. For any type of application, the material production is always the first experimental step. Among these 2D semiconductors, molybdenum disulfide ( $\text{MoS}_2$ ) is relatively more mature in terms of its synthesis technologies. Hence, in this paper, we provide a short literature survey of recent progresses in the synthesis of  $\text{MoS}_2$ . The paper focuses only on the production techniques rather than serving as a complete review on  $\text{MoS}_2$ -related physics, materials and electronics. Also, we put special emphasis on the recent achievements in metalorganic chemical vapor deposition (MOCVD) and atomic layer deposition (ALD), where gaseous precursors are used to grow  $\text{MoS}_2$ . It has a high potential for producing  $\text{MoS}_2$  with better quality and controllability for nanoelectronic device applications.

## 2. Synthesis Methods of $\text{MoS}_2$

$\text{MoS}_2$  has several polymorphs, where the 2H  $\text{MoS}_2$  has a layered hexagonal structure with lattice parameters of  $a = 0.316$  nm and  $c = 1.229$  nm [7], yielding an inter-layer spacing of 0.615 nm [8], as schematically shown in Figure 1. Bulk 2H  $\text{MoS}_2$  is an indirect bandgap semiconductor ( $\sim 1.29$  eV). With decreasing thickness, the bandgap increases. When it comes to monolayer  $\text{MoS}_2$ , it becomes a direct bandgap material, and the energy gap can be as large as  $\sim 1.90$  eV [9], suitable for fabricating most electronic devices. The synthesis methods of  $\text{MoS}_2$  can be divided into top-down and bottom-up approaches. We hereby describe them in turn.

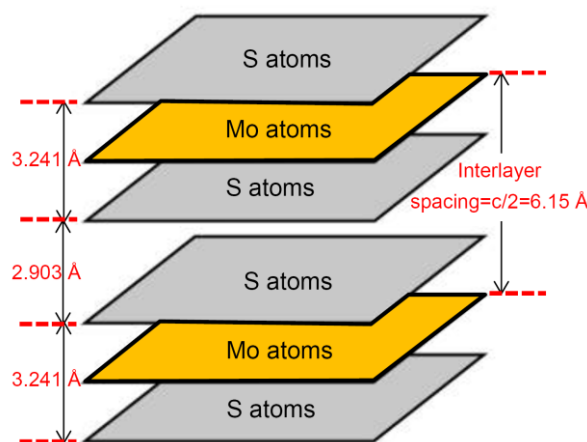


**Figure 1.** Distances between different layers in 2H  $\text{MoS}_2$ .

### 2.1. Top-down Approaches

#### 2.1.1. Micromechanical Exfoliation

Similar to the micromechanical exfoliation of graphene (a vivid lab demonstration can be found in [10]),  $\text{MoS}_2$  flakes can be produced on a substrate using sticky tapes. The starting material is bulk  $\text{MoS}_2$ , where some parts are peeled off with the tape and pressed into the substrate. Upon the release of the tape, some parts stay with the substrate rather than the tape due to the van der Waals force to the substrate. Repeating the process may produce flakes of  $\text{MoS}_2$  with random shapes, sizes and numbers of layers. This method offers 2D materials of the highest quality, enabling to study the pristine properties and ultimate device performances. For example, Kis et al. have used micro-exfoliation to produce  $\text{MoS}_2$  monolayers that are suitable for ultrasensitive photodetectors [11], analogue [12] and digital circuits [13], and observation of interesting physics such as mobility engineering and a

metal–insulator transition [14]. However, it was found that the van der Waals adhesion of many TMDs to  $\text{SiO}_2$ , a typical substrate, is much weaker than that of graphene. Therefore, the produced flakes are very small (typically  $<10\text{ }\mu\text{m}$ ) in their lateral size [15]. These results notwithstanding, large area  $\text{MoS}_2$  flakes can be exfoliated by slightly modifying the technique. Magda et al. obtained mono  $\text{MoS}_2$  layers with lateral size of several hundreds of microns by improving the  $\text{MoS}_2$ -substrate adhesion, as shown in Figure 2 [15]. The mechanism is that sulfur atoms can bind more strongly to gold than to  $\text{SiO}_2$ . The drawback is that such as-exfoliated  $\text{MoS}_2$  flakes have to be transferred to another new substrate, since in most applications the material is used on insulating substrates. In addition, like their graphene counterpart, the tape-assisted micromechanical exfoliation method offers very low yield, and it's not possible to scale up for large volume production, therefore  $\text{MoS}_2$  synthesized by this method is limited to fundamental study at lab scale.

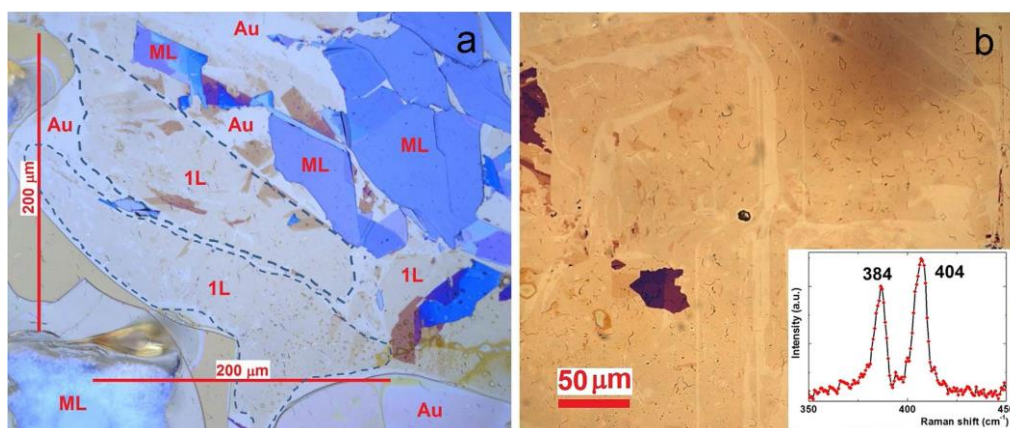


**Figure 2.** Large area  $\text{MoS}_2$  flakes exfoliated with chemically enhanced adhesion to the substrate [15].

### 2.1.2. Liquid Phase Exfoliation

Liquid phase exfoliation also starts from bulk  $\text{MoS}_2$ , producing flakes with random shapes, sizes and number of layers. The quantities, however, are much larger, and the quality lower. Roughly, there are 2 routes to exfoliate  $\text{MoS}_2$  in solution. The first is exfoliation by mechanical means such as sonication, shearing, stirring, grinding and bubbling [16–21]. The essence is purely physical, although some chemistry may still be involved [22–24]. For example, surfactants such as sodium deoxycholate (SDC) bile salt [22] and chitosan [23] may be added to the solution to prevent the exfoliated flakes from recombination. Electrolysis is employed to generate bubbles in some cases [24]. It is known that fine bubbles can squeeze into material interfaces and exfoliate them [25]. The yield of this method is dramatically improved from tape-assisted exfoliation, but the efficiency is still low for industrial applications. Therefore, a second route by atomic intercalation via solution chemistry [26] or electrochemistry [27] has been proposed. Lithium is typically used to intercalate between the  $\text{MoS}_2$  layers and enlarge the interlayer spacing, easing the following exfoliation by mechanical treatment (e.g., sonication). Fan et al. developed a process to exfoliate  $\text{MoS}_2$  nanosheets very efficiently using sonication assisted Li intercalation. They found that the complete Li intercalation with butyllithium can be effected within 1.5 hours [28]. An example of the  $\text{MoS}_2$  flakes synthesized by this method is shown in Figure 3. However, this method results in the loss of semiconducting properties due to the structural changes during Li intercalation. It is reported that above an annealing temperature of  $300\text{ }^\circ\text{C}$ , these  $\text{MoS}_2$  flakes can be somewhat recovered [26].

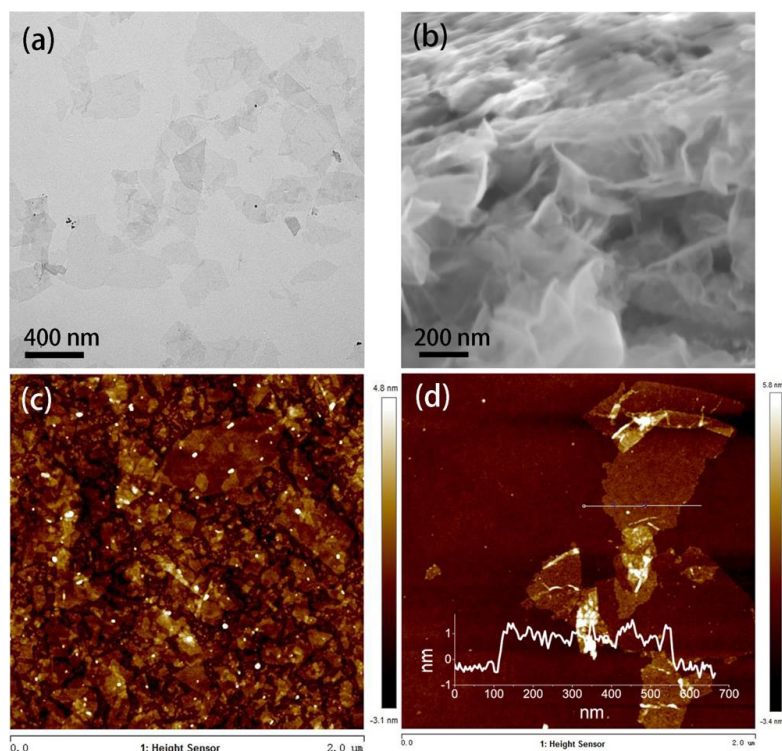


**Figure 3.** TEM, SEM and AFM images of MoS<sub>2</sub> flakes exfoliated by Li intercalation and sonication [28].

Liquid phase exfoliation is a simple technology with low cost, producing large quantity 2D nanosheets with relatively high quality. Therefore, it is regarded as the most suitable method for the large-scale industrial production of one- to few-layer 2D material flakes at low expense [29]. It is worth noting that liquid phase exfoliation can produce not only wet suspensions of flakes or dry powders, but macroscopically continuous thin films as well [30–32]. On substrates, through drop casting of the suspension and drying, MoS<sub>2</sub> thin films are prepared by Walia et al. [30–32], where optical and electrical properties can be studied.

## 2.2. Bottom-up Approaches

### 2.2.1. Physical Vapor Deposition

Although molecular beam epitaxy (MBE) is an advanced technology for growing single crystal semiconductor thin films, its application in producing 2D materials needs further development, and the grain size of the 2D material is not as high as expected [33]. In fact, even ordinary physical vapor deposition is rare. There is a report on growing MoS<sub>2</sub>-Ti composite by vacuum sputtering, using Ti and MoS<sub>2</sub> as the targets [34]. However, the MoS<sub>2</sub> is an amorphous structure in this case.

### 2.2.2. Solution Chemical Process

There are various methods for producing MoS<sub>2</sub> by solution chemistry. Hydrothermal synthesis [35] and solvothermal synthesis [36] typically use molybdate to react with sulfide or just sulfur in a stainless steel autoclave, where a series of physicochemical reactions take place under relatively high temperature (e.g., 200 °C) and high pressure for several hours or longer. The resultant is MoS<sub>2</sub> powders of different shapes. The size of individual particles can be adjusted to some extent. Very frequently, the powders are high-temperature post-annealed, to improve their crystalline quality and purity. The only difference between hydrothermal and solvothermal synthesis is that the precursor solution in the latter case is usually not aqueous. Other solution chemical processes start at almost room temperature and atmospheric pressure, where post-annealing is often used anyway [37–41].



The products can be either a powder or thin film, depending on the preparation details. The most commonly-used precursor is  $(\text{NH}_4)_2\text{MoS}_4$  (ammonium tetrathiomolybdate), or something similar.  $(\text{NH}_4)_2\text{MoS}_4$  decomposes to form  $\text{MoO}_3$  at 120–360 °C, which can be further converted into  $\text{MoS}_2$ . In some cases, electrochemical deposition [42–44] and photo-assisted deposition are used [45]. For instance, Li et al. fabricated  $\text{MoS}_2$  nanowires and nanoribbons using  $\text{MoO}_x$  as the precursor [43]. The  $\text{MoO}_x$  precursor is then exposed to  $\text{H}_2\text{S}$  at high temperature (500–800 °C) to synthesize  $\text{MoS}_2$ . Depending on the temperature for processing, both 2H and 3R phase of  $\text{MoS}_2$  can be synthesized. The  $\text{MoS}_2$  nanoribbons can be 50  $\mu\text{m}$  in length and are aligned in parallel arrays which are preferable for device fabrication, as shown in Figure 4.

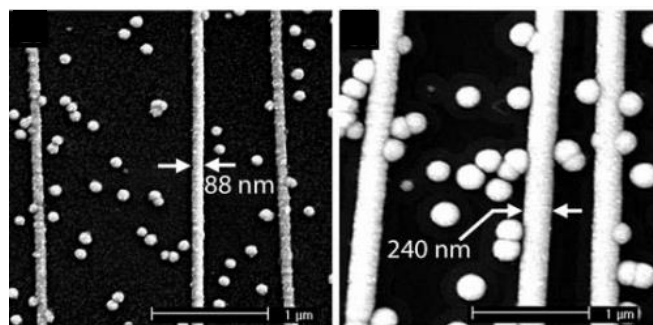
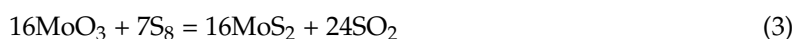
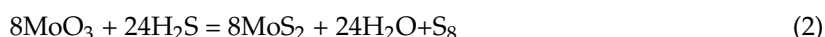
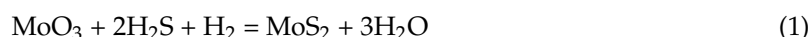


**Figure 4.**  $\text{MoS}_2$  nanowires/nanoribbons synthesized from  $\text{MoO}_x$  precursor [43].

### 2.2.3. Chemical Vapor Deposition (CVD)

Among all the synthesis methods, CVD is the most compatible to existing semiconductor technology. Typically, it forms the film on a substrate, where chemical reactions are involved in the growth mechanism. The large-area growth of highly uniform  $\text{MoS}_2$  will enable the batch fabrication of atomically thin devices and circuitry. Currently, most works start with solid state precursors of molybdenum, such as  $\text{MoO}_3$  [46,47] or  $\text{Mo}$  [48]. If the  $\text{Mo}$  precursors are not vaporized in the process, often the technique is also called sulfurization [46–48]. Typical S precursors are  $\text{H}_2\text{S}$  gas [49] or vaporized S [46–48,50]. It is argued that using  $\text{MoCl}_5$  precursors are easier to achieve monolayer  $\text{MoS}_2$  over large area [50]. Earlier, the  $\text{MoS}_2$  could be noncontinuous [47], which is not a big problem nowadays. The usual growth temperatures are 700–1000 °C, and the inclusion of a metal catalyst such as Au is favorable for the film quality [49]. Typical reactions taking place in the CVD are one of these:



With plasma-enhanced chemical vapor deposition (PECVD), the growth temperature of  $\text{MoS}_2$  can be lowered to 150–300 °C, making it possible to directly deposit  $\text{MoS}_2$  even on plastic substrates [51].

Metal-organic CVD is a special case of CVD where organometallic precursors are used. It is used in the modern semiconductor industry to produce single crystal epitaxial films. Recently, a few reports have appeared on the application of this method in the growth of  $\text{MoS}_2$  thin films [49,52–54]. Kang et al. [52] have grown  $\text{MoS}_2$  and  $\text{WS}_2$  on 4-inch oxidized silicon wafers by MOCVD. The  $\text{MoS}_2$  is grown with gaseous precursors of  $\text{Mo}(\text{CO})_6$  (boiling point 156 °C) and  $(\text{C}_2\text{H}_5)_2\text{S}$ . At 550 °C, monolayer  $\text{MoS}_2$  with full coverage of the substrate (typically  $\text{SiO}_2/\text{Si}$  and fused silica) is deposited for  $t_0 \sim 26$  h. Figure 5a shows scanning electron microscopy (SEM) images of the samples, demonstrating the effect of adding  $\text{H}_2$  in the gas mixture. It is argued that  $\text{H}_2$  enhances the decomposition of  $(\text{C}_2\text{H}_5)_2\text{S}$  (increasing nucleation due to hydrogenolysis) and etches  $\text{MoS}_2$  (preventing intergrain connection) [52]. It seems that a low  $\text{H}_2$  rate is beneficial for growing continuous monolayer  $\text{MoS}_2$ . Nevertheless,  $\text{H}_2$  is

necessary for removing the carbonaceous species generated during the MOCVD. Therefore, the  $H_2$  flow should be optimized. To have successful growth, dehydrating the growth environment is also necessary. Figure 5b indicates that the growth mode is layer-by-layer under this specific condition. When  $t < t_0$  there is almost no nucleation of the second  $MoS_2$  layer, which takes place mainly at the grain boundaries of the first layer when  $t > t_0$ . Figure 5c shows a top gated ( $V_{TG}$ )  $MoS_2$  transistor with a field-effect mobility of  $29 \text{ cm}^2 \text{ V}^{-1} \text{ s}^{-1}$  and transconductance  $2 \text{ } \mu\text{S}/\mu\text{m}$ , determined from the transfer properties. The current saturation occurs at relatively low  $V_{SD}$  (see the inset). These features compete well with the state-of-the-art  $MoS_2$  transistors. Figure 5d–f demonstrates the optical absorption, Raman and photoluminescence spectra measured from the MOCVD grown  $MoS_2$  (and  $WS_2$ ) films, respectively, where the features agree well with the characteristics of exfoliated monolayer counterparts (denoted by diamonds).

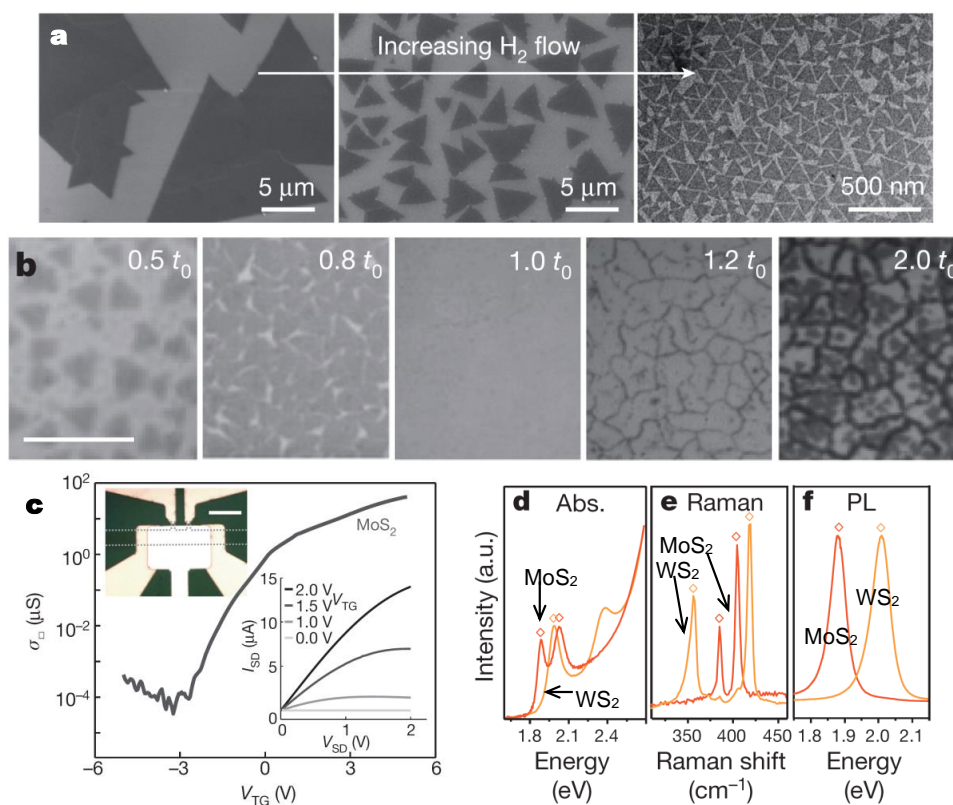


**Figure 5.** (a) Grain size evolution of monolayer  $MoS_2$  as a function of  $H_2$  flow. From left to right, 5, 20 and 200 sccm  $H_2$ . (b) Optical images of  $MoS_2$  films as a function of growth time.  $t_0$  is the optimal time for full monolayer coverage ( $\sim 26$  h). (c) Transfer and output properties of the field-effect transistor fabricated in the MOCVD grown  $MoS_2$  with top gate configuration.  $\sigma_{\square}$  denotes sheet conductance. Scale bar: 10  $\mu\text{m}$ . (d–f) Optical absorption, Raman and normalized photoluminescence spectra of as-grown monolayer  $MoS_2$  (red) and  $WS_2$  (orange) films. The peak positions in (d–f) are consistent with exfoliated flakes (denoted by diamonds) [52].

At this stage, the material quality in [53] is still too low to be competitive. The large-area deposition of monolayer  $MoS_2$  as well as other TMDs with spatial homogeneity and high performance is still challenging.  $MoS_2$  films today are polycrystalline with the grain size typically ranging from 1 to 10 micrometers. This notwithstanding, the MOCVD synthesis of 2D semiconductors indeed opens a pathway towards future exciting nanoelectronic materials. The most important reason for this is that, in MOCVD, ultrapure gaseous precursors are injected into the reactor and finely dosed to deposit a very thin layer of atoms onto the substrate. Even if a solid or liquid precursor is used, it will be vaporized in situ in the chamber [53]. Unlike solid and liquid precursors, here the building-blocks for

growing the film are much finer, naturally leading to better quality and controllability. The heated metalorganic precursor molecules decompose via pyrolysis, leaving the atoms on the substrate. The atoms bond to the surface, and an ultrathin MoS<sub>2</sub> layer is grown.

Based on this argument, one can easily think of another promising synthesis method: ALD [55], which can be seen as a subclass of CVD. In ALD, the film is grown by exposing the substrate surface to alternating gas precursors. In contrast to ordinary CVD, the precursors are never simultaneously present in the chamber. Instead, they are introduced as sequential and non-overlapping pulses, separated by purges in between. In each pulse, molecules react with the surface in a self-limiting way. Hence, it is possible to grow materials with high-thickness precision (layer by layer). Indeed, very recently, people have used ALD to grow MoS<sub>2</sub>, such as in [56]. Using MoCl<sub>5</sub> (vaporized) and H<sub>2</sub>S precursors, monolayer to few-layer MoS<sub>2</sub> on large SiO<sub>2</sub>/Si or quartz substrates is obtained [56]. In the photos of two 150 mm quartz wafers before and after the ALD, the substrate changes to dark yellow uniformly (~2 layers of MoS<sub>2</sub>) [56]. It is found that photoresist residues on the surface lead to more nucleation sites for MoS<sub>2</sub>, but this mechanism remains to be confirmed. Figure 6a plots Raman signals for 50 cycle ALD MoS<sub>2</sub>, where the E<sub>2g</sub><sup>1</sup> and A<sub>1g</sub> characteristic peaks are sharper and higher for 475 °C deposition temperature, indicating its higher material quality. After the ALD, some samples are annealed in a sulfur environment (H<sub>2</sub>S or S atmosphere). Figure 6b shows that after sulfur annealing at increasingly high temperature, the characteristic peaks get narrower, stronger and more symmetric. After annealing at 920 °C, the full width at half maximum of the E<sub>2g</sub><sup>1</sup> peak is close to that of exfoliated MoS<sub>2</sub> monolayer (4.2 cm<sup>-1</sup> vs. 3.7 cm<sup>-1</sup>). By analyzing the separation  $\Delta$  between E<sub>2g</sub><sup>1</sup> and A<sub>1g</sub> peaks, one can tentatively determine the number of layers in MoS<sub>2</sub> films [56]. In Figure 6c, the sample grown at 475 °C and annealed at 920 °C seems to be 1–2 monolayers. Future electronic measurements are needed to further examine the film quality.

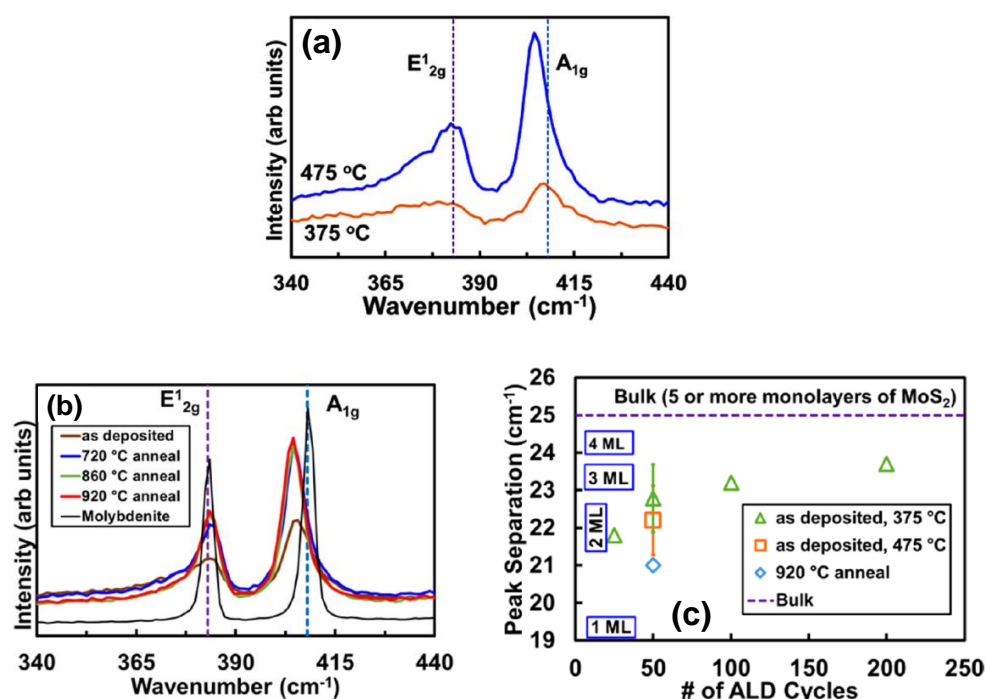


**Figure 6.** (a) Raman spectroscopy measurements of ALD MoS<sub>2</sub> at 375 or 475 °C, where the latter shows higher quality. (b) Raman spectra of 475 °C deposited MoS<sub>2</sub> films (some are post annealed in sulfur environment), where 920 °C annealing leads to the best quality. The curve for bulk MoS<sub>2</sub> is for reference. (c) E<sub>2g</sub><sup>1</sup> to A<sub>1g</sub> peak separation  $\Delta$  plotted against the cycle number in ALD.  $\Delta \sim 19$  cm<sup>-1</sup> tentatively indicates MoS<sub>2</sub> monolayer, whereas bulk (>5 layers) material has  $\Delta \sim 25$  cm<sup>-1</sup> [56].



### 3. Conclusions

In this paper, we have reviewed the synthesis methods of MoS<sub>2</sub> in terms of top-down and bottom-up approaches. Micromechanical exfoliation offers the highest material quality but is limited by the yield so it is mainly for basic research, whereas liquid phase exfoliation and solution chemical process are of low cost, with decent material quality and suitable for large-scale industrial production. MoS<sub>2</sub> thin films aiming for high-end electronic applications are produced by CVD. In this review, we have put a special emphasis on the MOCVD and ALD methods, because they are more sophisticated technology with gas phase precursors and will most likely be the dominant techniques in producing MoS<sub>2</sub> films oriented towards real electronic device applications in the future. In most cases the MoS<sub>2</sub> films are transfer-free, which is vital for industrial applications that require a high process controllability and reproducibility [57]. At the moment, production of MoS<sub>2</sub> as a high quality electronic material is still challenging. This notwithstanding, most of the reviewed processes can be extended to other 2D materials (with some modification), and with future technological advances, the successful production of advanced 2D nanoelectronic materials can be envisioned.

**Acknowledgments:** We would like to thank National Natural Science Foundation of China (11674016), National key R & D program (2017YFB0403100), Beijing Natural Science Foundation (4152003), Beijing Municipal Commission of Education (PXM2016\_014204\_500018), and Swedish Foundation for International Cooperation in Research and Higher Education (CH2015-6202).

**Author Contributions:** J. Sun, X. Li and Y. Fu wrote the paper, led the discussion and summarized the literature; W. Guo, M. Zhao, C. Xu and J. Deng participated in the discussion; X. Fan and Y. Dong helped to summarize the literature.

**Conflicts of Interest:** The authors declare no conflict of interest.

### References

1. Ferrari, A.C.; Bonaccorso, F.; Fal'Ko, V.; Novoselov, K.S.; Roche, S.; Bøggild, P.; Borini, S.; Koppens, F.H.; Palermo, V.; Pugno, N.; et al. Science and technology roadmap for graphene, related two-dimensional crystals, and hybrid systems. *Nanoscale* **2015**, *7*, 4598–4810. [CrossRef] [PubMed]
2. Novoselov, K.S.; Geim, A.K.; Morozov, S.V.; Jiang, D.; Zhang, Y.; Dubonos, S.V.; Grigorieva, I.V.; Firsov, A.A. Electric field effect in atomically thin carbon films. *Science* **2004**, *306*, 666–669. [CrossRef] [PubMed]
3. Xu, K.; Xu, C.; Deng, J.; Zhu, Y.; Guo, W.; Mao, M.; Zheng, L.; Sun, J. Graphene transparent electrodes grown by rapid chemical vapor deposition with ultrathin indium tin oxide contact layers for GaN light emitting diodes. *Appl. Phys. Lett.* **2013**, *102*, 162102.
4. Li, L.; Yu, Y.; Ye, G.J.; Ge, Q.; Ou, X.; Wu, H.; Feng, D.; Chen, X.H.; Zhang, Y. Black phosphorus field-effect transistors. *Nature Nanotechnol.* **2014**, *9*, 372–377. [CrossRef] [PubMed]
5. Chhowalla, M.; Shin, H.S.; Eda, G.; Li, L.J.; Loh, K.P.; Zhang, H. The chemistry of two-dimensional layered transition metal dichalcogenide nanosheets. *Nature Chem.* **2013**, *5*, 263–275. [CrossRef] [PubMed]
6. Al Balushi, Z.Y.; Wang, K.; Ghosh, R.K.; Vilá, R.A.; Eichfeld, S.M.; Caldwell, J.D.; Qin, X.; Lin, Y.C.; DeSario, P.A.; Stone, G.; et al. Two-dimensional gallium nitride realized via graphene encapsulation. *Nature Mater.* **2016**, *15*, 1166–1171. [CrossRef] [PubMed]
7. Stewart, J.A.; Spearot, D.E. Atomistic simulations of nanoindentation on the basal plane of crystalline molybdenum disulfide (MoS<sub>2</sub>). *Model. Simul. Mater. Sci. Eng.* **2013**, *21*, 045003. [CrossRef]
8. Ai, K.; Ruan, C.; Shen, M.; Lu, L. MoS<sub>2</sub> nanosheets with widened interlayer spacing for high-efficiency removal of mercury in aquatic systems. *Adv. Funct. Mater.* **2016**, *26*, 5542–5549. [CrossRef]
9. Splendiani, A.; Sun, L.; Zhang, Y.; Li, T.; Kim, J.; Chim, C.-Y.; Galli, G.; Wang, F. Emerging photoluminescence in monolayer MoS<sub>2</sub>. *Nano Lett.* **2010**, *10*, 1271–1275. [CrossRef] [PubMed]
10. Vivid Lab Demonstration. Available online: <https://www.youtube.com/watch?v=9l5d0YLZgec&feature=youtu.be> (accessed on 30 June 2017).
11. Lopez-Sanchez, O.; Lembke, D.; Kayci, M.; Radenovic, A.; Kis, A. Ultrasensitive photodetectors based on monolayer MoS<sub>2</sub>. *Nature Nanotechnol.* **2013**, *8*, 497–501. [CrossRef] [PubMed]

12. Radisavljevic, B.; Whitwick, M.B.; Kis, A. Small-signal amplifier based on single-layer MoS<sub>2</sub>. *Appl. Phys. Lett.* **2012**, *101*, 043103. [[CrossRef](#)]
13. Radisavljevic, B.; Whitwick, M.B.; Kis, A. Integrated circuits and logic operations based on single-layer MoS<sub>2</sub>. *ACS Nano* **2011**, *5*, 9934–9938. [[CrossRef](#)] [[PubMed](#)]
14. Radisavljevic, B.; Kis, A. Mobility engineering and a metal–insulator transition in monolayer MoS<sub>2</sub>. *Nat. Mater.* **2013**, *12*, 815–820. [[CrossRef](#)] [[PubMed](#)]
15. Magda, G.; Pető, J.; Dobrik, G.; Hwang, C.; Biró, L.; Tapasztó, L. Exfoliation of large-area transition metal chalcogenide single layers. *Sci. Rep.* **2015**, *5*, 14714. [[CrossRef](#)] [[PubMed](#)]
16. Forsberg, V.; Zhang, R.; Bäckström, J.; Dahlström, C.; Andres, B.; Norgren, M.; Andersson, M.; Hummelgård, M.; Olin, H. Exfoliated MoS<sub>2</sub> in Water without Additives. *PLoS ONE* **2016**, *11*, 0154522. [[CrossRef](#)] [[PubMed](#)]
17. Gupta, A.; Arunachalam, V.; Vasudevan, S. Liquid-phase exfoliation of MoS<sub>2</sub> nanosheets: The critical role of trace water. *J. Phys. Chem. Lett.* **2016**, *7*, 4884–4890. [[CrossRef](#)] [[PubMed](#)]
18. Yao, Y.; Lin, Z.; Li, Z.; Song, X.; Moon, K.-S.; Wong, C.-p. Large-scale production of two-dimensional nanosheets. *J. Mater. Chem.* **2012**, *22*, 13494–13499. [[CrossRef](#)]
19. Yu, Y.; Jiang, S.; Zhou, W.; Miao, X.; Zeng, Y.; Zhang, G.; Liu, S. Room temperature rubbing for few-layer two-dimensional thin flakes directly on flexible polymer substrates. *Sci. Rep.* **2013**, *3*, 2697. [[CrossRef](#)] [[PubMed](#)]
20. Varrla, E.; Backes, C.; Paton, K.; Harvey, A.; Gholamvand, Z.; McCauley, J.; Coleman, J. Large-scale production of size-controlled MoS<sub>2</sub> nanosheets by shear exfoliation. *Chem. Mater.* **2015**, *27*, 1129–1139. [[CrossRef](#)]
21. Paton, K.; Varrla, E.; Backes, C.; Smith, R.J.; Khan, U.; O'Neill, A.; Boland, C.; Lotya, M.; Istrate, O.M.; King, P.; et al. Scalable production of large quantities of defect-free few-layer graphene by shear exfoliation in liquids. *Nature Mater.* **2014**, *13*, 624–630. [[CrossRef](#)] [[PubMed](#)]
22. Zhang, M.; Howe, R.; Woodward, R.; Kelleher, E.; Torrisi, F.; Hu, G.; Popov, S.; Taylor, J.; Hasan, T. Solution processed MoS<sub>2</sub>-PVA composite for sub-bandgap mode-locking of a wideband tunable ultrafast Er:fiber laser. *Nano Res.* **2015**, *8*, 1522–1534. [[CrossRef](#)]
23. Zhang, W.; Wang, Y.; Zhang, D.; Yu, S.; Zhu, W.; Wang, J.; Zheng, F.; Wang, S.; Wang, J. A one-step approach to the large-scale synthesis of functionalized MoS<sub>2</sub> nanosheets by ionic liquid assisted grinding. *Nanoscale* **2015**, *7*, 10210–10217. [[CrossRef](#)] [[PubMed](#)]
24. Liu, N.; Kim, P.; Kim, J.; Ye, J.; Kim, S.; Lee, C. Large-area atomically thin MoS<sub>2</sub> nanosheets prepared using electrochemical exfoliation. *ACS Nano* **2014**, *8*, 6902–6910. [[CrossRef](#)] [[PubMed](#)]
25. Liu, L.; Liu, X.; Zhan, Z.; Guo, W.; Xu, C.; Deng, J.; Chakarov, D.; Hyldgaard, P.; Schröder, E.; Yurgens, A.; Sun, J. A mechanism for highly efficient electrochemical bubbling delamination of CVD-grown graphene from metal substrates. *Adv. Mater. Interf.* **2016**, *3*, 1500492. [[CrossRef](#)]
26. Eda, G.; Yamaguchi, H.; Voiry, D.; Fujita, T.; Chen, M.; Chhowalla, M. Photoluminescence from chemically exfoliated MoS<sub>2</sub>. *Nano Lett.* **2011**, *11*, 5111–5116. [[CrossRef](#)] [[PubMed](#)]
27. Zeng, Z.; Yin, Z.; Huang, X.; Li, H.; He, Q.; Lu, G.; Boey, F.; Zhang, H. Single layer semiconducting nanosheets: High-yield preparation and device fabrication. *Angew. Chem. Int. Ed.* **2011**, *50*, 11093–11097. [[CrossRef](#)] [[PubMed](#)]
28. Fan, X.; Xu, P.; Zhou, D.; Sun, Y.; Li, Y.; Nguyen, M.; Terrones, M.; Mallouk, T. Fast and efficient preparation of exfoliated 2H MoS<sub>2</sub> nanosheets by sonication-assisted lithium intercalation and infrared laser-induced 1T to 2H phase reversion. *Nano Lett.* **2015**, *15*, 5956–5960. [[CrossRef](#)] [[PubMed](#)]
29. Coleman, J.; Lotya, M.; O'Neill, A.; Bergin, S.D.; King, P.J.; Khan, U.; Young, K.; Gaucher, A.; De, S.; Smith, R.J.; et al. Two-dimensional nanosheets produced by liquid exfoliation of layered materials. *Science* **2011**, *331*, 568–571. [[CrossRef](#)] [[PubMed](#)]
30. Rezk, A.R.; Walia, S.; Ramanathan, R.; Nili, H.; Ou, J.Z.; Bansal, V.; Friend, J.R.; Bhaskaran, M.; Yeo, L.Y.; Sriram, S. Acoustic–excitonic coupling for dynamic photoluminescence manipulation of quasi-2D MoS<sub>2</sub> nanoflakes. *Adv. Opt. Mater.* **2015**, *3*, 888–894. [[CrossRef](#)]

31. Balendhran, S.; Walia, S.; Nili, H.; Ou, J.Z.; Zhuiykov, S.; Kaner, R.B.; Sriram, S.; Bhaskaran, M.; Kalantar-zadeh, K. Two-dimensional molybdenum trioxide and dichalcogenides. *Adv. Funct. Mater.* **2013**, *23*, 3952–3970. [[CrossRef](#)]
32. Walia, S.; Balendhran, S.; Wang, Y.; Kadir, R.A.; Zoolfakar, A.S.; Atkin, P.; Ou, J.Z.; Sriram, S.; Kalantar-zadeh, K.; Bhaskaran, M. Characterization of metal contacts for two-dimensional MoS<sub>2</sub> nanoflakes. *Appl. Phys. Lett.* **2013**, *103*, 232105. [[CrossRef](#)]
33. Vishwanath, S.; Liu, X.; Rouvimov, S.; Mende, P.; Azcatl, A.; McDonnell, S.; Wallace, R.; Feenstra, R.; Furdyna, J.; Jena, D.; Xing, H. Comprehensive structural and optical characterization of MBE grown MoSe<sub>2</sub> on graphite, CaF<sub>2</sub> and graphene. *2D Mater.* **2015**, *2*, 024007. [[CrossRef](#)]
34. Qin, X.; Ke, P.; Wang, A.; Kim, K. Microstructure, mechanical and tribological behaviors of MoS<sub>2</sub>-Ti composite coatings deposited by a hybrid HIPIMS method. *Surf. Coat. Technol.* **2013**, *228*, 275–281. [[CrossRef](#)]
35. Zhou, X.; Xu, B.; Lin, Z.; Shu, D.; Ma, L. Hydrothermal synthesis of flower-like MoS<sub>2</sub> nanospheres for electrochemical supercapacitors. *J. Nanosci. Nanotechnol.* **2014**, *14*, 7250–7254. [[CrossRef](#)] [[PubMed](#)]
36. Feng, X.; Tang, Q.; Zhou, J.; Fang, J.; Ding, P.; Sun, L.; Shi, L. Novel mixed-solvothermal synthesis of MoS<sub>2</sub> nanosheets with controllable morphologies. *Cryst. Res. Technol.* **2013**, *48*, 363–368. [[CrossRef](#)]
37. Liao, H.; Wang, Y.; Zhang, S.; Qian, Y. A solution low-temperature route to MoS<sub>2</sub> fiber. *Chem. Mater.* **2011**, *13*, 6–8. [[CrossRef](#)]
38. Li, X.; Zhang, W.; Wu, Y.; Min, C.; Fang, J. Solution-processed MoS<sub>x</sub> as an efficient anode buffer layer in organic solar cells. *ACS Appl. Mater. Interf.* **2013**, *5*, 8823–8827. [[CrossRef](#)] [[PubMed](#)]
39. Liu, K.K.; Zhang, W.; Lee, Y.-H.; Lin, Y.-C.; Chang, M.-T.; Su, C.-Y.; Chang, C.-S.; Li, H.; Shi, Y.; Zhang, H.; Lai, C.-S.; Li, L.-J. Growth of large-area and highly crystalline MoS<sub>2</sub> thin layers on insulating substrates. *Nano Lett.* **2012**, *12*, 1538–1544. [[CrossRef](#)] [[PubMed](#)]
40. Bezverkhy, I.; Afanasiev, P.; Lacroix, M. Aqueous preparation of highly dispersed molybdenum sulfide. *Inorg. Chem.* **2000**, *39*, 5416–5417. [[CrossRef](#)] [[PubMed](#)]
41. Afanasiev, P.; Geantet, C.; Thomozeau, C.; Jouget, B. Molybdenum polysulfide hollow microtubules grown at room temperature from solution. *Chem. Commun.* **2000**, *12*, 1001–1002. [[CrossRef](#)]
42. Maijenburg, A.; Regis, M.; Hattori, A.; Tanaka, H.; Choi, K.-S.; ten Elshof, J. MoS<sub>2</sub> nanocube structures as catalysts for electrochemical H<sub>2</sub> evolution from acidic aqueous solutions. *ACS Appl. Mater. Interf.* **2014**, *6*, 2003–2010. [[CrossRef](#)] [[PubMed](#)]
43. Li, Q.; Walter, E.; van der Veer, W.; Murray, B.; Newberg, J.; Bohannon, E.; Switzer, J.; Hemminger, J.; Penner, R. Molybdenum disulfide nanowires and nanoribbons by electrochemical/chemical synthesis. *J. Phys. Chem. B* **2005**, *109*, 3169–3182. [[CrossRef](#)] [[PubMed](#)]
44. Kibsgaard, J.; Chen, Z.; Reinecke, B.; Jaramillo, T. Engineering the surface structure of MoS<sub>2</sub> to preferentially expose active edge sites for electrocatalysis. *Nature Mater.* **2012**, *11*, 963–969. [[CrossRef](#)] [[PubMed](#)]
45. Nguyen, M.; Tran, P.; Pramana, S.; Lee, R.; Batabyal, S.; Mathews, N.; Wong, L.; Graetzel, M. In situ photo-assisted deposition of MoS<sub>2</sub> electrocatalyst onto zinc cadmium sulphide nanoparticle surfaces to construct an efficient photocatalyst for hydrogen generation. *Nanoscale* **2013**, *5*, 1479–1482. [[CrossRef](#)] [[PubMed](#)]
46. Lin, Y.-C.; Zhang, W.; Huang, J.-K.; Liu, K.-K.; Lee, Y.-H.; Liang, C.-T.; Chu, C.-W.; Li, L.-J. Wafer-scale MoS<sub>2</sub> thin layers prepared by MoO<sub>3</sub> sulfurization. *Nanoscale* **2012**, *4*, 6637–6641. [[CrossRef](#)] [[PubMed](#)]
47. Cai, J.; Jian, J.; Chen, X.; Lei, M.; Wang, W. Regular hexagonal MoS<sub>2</sub> microflakes grown from MoO<sub>3</sub> precursor. *Appl. Phys. A* **2007**, *89*, 783–788. [[CrossRef](#)]
48. Zhan, Y.; Liu, Z.; Najmaei, S.; Ajayan, P.; Lou, J. Large-area vapor-phase growth and characterization of MoS<sub>2</sub> atomic layers on a SiO<sub>2</sub> substrate. *Small* **2014**, *8*, 966–971. [[CrossRef](#)] [[PubMed](#)]
49. Song, I.; Park, C.; Hong, M.; Baik, J.; Shin, H.-J.; Choi, H. Patternable large-scale molybdenum disulfide atomic layers grown by gold-assisted chemical vapor deposition. *Angew. Chem. Int. Ed.* **2014**, *53*, 1266–1269. [[CrossRef](#)] [[PubMed](#)]
50. Yu, Y.; Li, C.; Liu, Y.; Su, L.; Zhang, Y.; Cao, L. Controlled scalable synthesis of uniform, high-quality monolayer and few-layer MoS<sub>2</sub> Films. *Sci. Rep.* **2013**, *3*, 1866. [[CrossRef](#)] [[PubMed](#)]
51. Ahn, C.; Lee, J.; Kim, H.-U.; Bark, H.; Jeon, M.; Ryu, G.; Lee, Z.; Yeom, G.; Kim, K.; Jung, J.; Kim, Y.; Lee, C.; Kim, T. Low-temperature synthesis of large-scale molybdenum disulfide thin films directly on a plastic substrate using plasma-enhanced chemical vapor deposition. *Adv. Mater.* **2015**, *27*, 5223–5229. [[CrossRef](#)] [[PubMed](#)]

52. Kang, K.; Xie, S.; Huang, L.; Han, Y.; Huang, P.; Mak, K.; Kim, C.-J.; Muller, D.; Park, J. High-mobility three-atom-thick semiconducting films with wafer-scale homogeneity. *Nature* **2015**, *520*, 656–660. [[CrossRef](#)] [[PubMed](#)]
53. Olofinjana, B.; Egharevba, G.; Taleatu, B.; Akinwunmi, O.; Ajayi, E. MOCVD of molybdenum sulphide thin film via single solid source precursor bis-(morpholinodithioato-s,s')-Mo. *J. Mod. Phys.* **2011**, *2*, 341–349. [[CrossRef](#)]
54. Kumar, V.; Dhar, S.; Choudhury, T.; Shivashankar, S.; Raghavan, S. A predictive approach to CVD of crystalline layers of TMDs: The case of MoS<sub>2</sub>. *Nanoscale* **2015**, *7*, 7802–7810. [[CrossRef](#)] [[PubMed](#)]
55. Sun, J.; Larsson, M.; Maximov, I.; Hardtdegen, H.; Xu, H. Gate-defined quantum-dot devices realized in InGaAs/InP by incorporating a HfO<sub>2</sub> layer as gate dielectric. *Appl. Phys. Lett.* **2009**, *94*, 042114. [[CrossRef](#)]
56. Valdivia, A.; Tweet, D.; Conley, J., Jr. Atomic layer deposition of two dimensional MoS<sub>2</sub> on 150 mm substrates. *J. Vac. Sci. Technol. A* **2016**, *34*, 021515. [[CrossRef](#)]
57. Sun, J.; Cole, M.; Lindvall, N.; Teo, K.; Yurgens, A. Noncatalytic chemical vapor deposition of graphene on high-temperature substrates for transparent electrodes. *Appl. Phys. Lett.* **2012**, *100*, 022102.



© 2017 by the authors. Licensee MDPI, Basel, Switzerland. This article is an open access article distributed under the terms and conditions of the Creative Commons Attribution (CC BY) license (<http://creativecommons.org/licenses/by/4.0/>).